ANNALI DI GEOFISICA, VOL. 42, N. 2, April 1999

Satellite mapping of the Antarctic gravity field

Ralph R.B. von Frese ([1]), **Daniel R. Roman** ([1]), **Jeong-Hee Kim** ([2]), **Jeong Woo Kim** ([3]) **and Allen J. Anderson** ([4])

([1]) *Byrd Polar Research Center and Department of Geological Sciences, The Ohio State University, Columbus, OH 43210, U.S.A.*

([2]) *Department of Civil Engineering, Kyongnam National University, Republic of Korea*

([3]) *Department of Earth Sciences, Sejong University, Republic of Korea*

([4]) *Department of Physics, University of California-Santa Barbara, CA 93106, U.S.A.*

Abstract

The production and analysis of the Antarctic digital magnetic anomaly map will be greatly aided by complementary gravity data. They help to constrain thickness variations of the crust and related magnetic effects that may be used for correcting long-wavelength errors in near-surface magnetic survey compilations. They also limit ambiguities in geological interpretations of magnetic anomalies. Antarctic free-air gravity anomalies are available from the 1° Earth Gravity Model 1996 (EGM96). These coefficients satisfy gravity estimates from satellite radar altimetry, as well as surface or near-surface measurements in roughly 75% of the 30 arc-minute blocks south of 60°S. For the remaining blocks, the EGM96 predictions are limited in resolution to degree 70 based on satellite orbital analyses. Anomaly predictions over the unsurveyed regions of the Antarctic will be greatly improved by additional orbital measurements from the pending low-altitude (*i.e.*, 150-500 km) CHAMP and GRACE satellite missions of ESA and NASA, respectively. Shorter wavelength anomalies are available from Geosat and ERS-1 & 2 radar altimetry data for marine regions away from the shoreline that compare very well with modern, good-quality shipborne data. Over the Gunnerus Ridge region, for example, satellite altimetry-derived free-air gravity predictions at a 3-5 km grid interval have an accuracy of about 3 mgals or less.

Key words *ADMAP – gravity – Antarctic – satellite – altimetry*

1. Introduction

Antarctic gravity anomalies provide constraints on subsurface variations of mass that are important for understanding the evolution of the Antarctic crust, mantle, and core. These data are particularly critical for crustal studies of the Antarctic where much less than 1% of the region offers surface outcrops for direct geological field study, because of the ubiquitous cover of snow, ice and sea water. Gravity anomalies also complement subglacial interpretations of magnetic anomaly data because crustal variations in composition, structure and heat flow are commonly reflected in correlative density and magnetization contrasts (*e.g.*, Chandler *et al.*, 1981; von Frese *et al.*, 1982, 1997a).

Gravity anomaly data also may facilitate extracting the crustal components in magnetic observations. For example, combining free-air gravity anomalies with an effective gravity model of the terrain can yield a model of crustal thickness variations (von Frese *et al.*, 1999a). The pseudo-magnetic effects of this model may then

Mailing address: Prof. Ralph R.B. von Frese, Department of Geological Sciences, The Ohio State University, 125 South Oval Mall, Columbus, Ohio 43210-1398, U.S.A.; e-mail: vonfrese@geology.ohio.state.edu

be obtained via Poisson's theorem for enhanced separation of crustal and core field effects (von Frese *et al.*, 1999b). In this way, gravity data may facilitate the development of a crustal magnetic reference map from satellite magnetic observations that can be useful for correcting long-wavelength errors in Antarctic compilations of disparate near-surface magnetic surveys (von Frese *et al.*, 1999b).

The properties of the Antarctic gravity field are largely derived from satellite observations because near-surface observations have been very limited due to the great cost and severe restrictions of doing polar field work. Satellite studies of the gravity field began in the early 1960's when the motions of satellites were used to estimate low-order gravity field variations. Since the 1980's, with the introduction of spaceborne altimetry, precise laser tracking systems, and the Global Positioning System (GPS), our ability to estimate the higher order components of the Earth's gravity field has improved markedly.

Figure 1 shows 1° predictions of Antarctic free-air gravity anomalies from the spherical harmonic expansion of the most current Earth Gravity Model 1996 (Lemoine *et al.*, 1998). They are evaluated at an altitude that is somewhat greater than the 111 km wavelength resolution implied

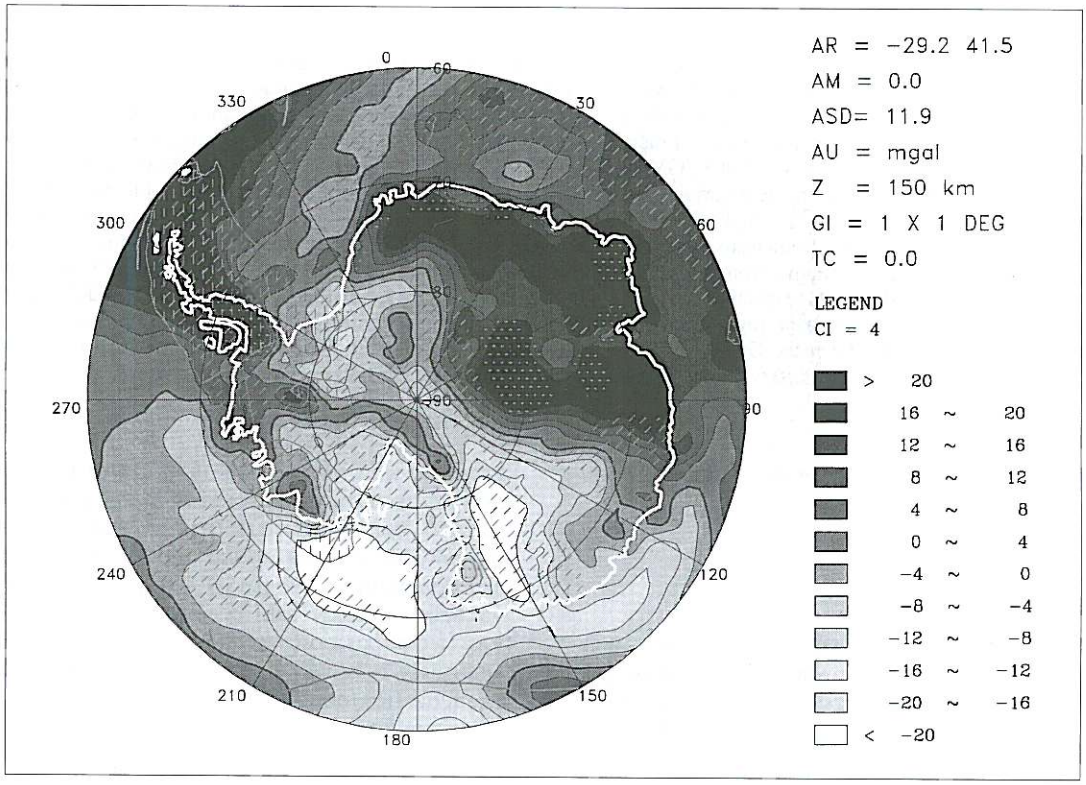

Fig. 1. Antarctic Free-Air Gravity Anomalies (FAGA) at 150 km altitude from the EGM96 spherical harmonic coefficients to degree and order 360. Annotations include the Amplitude Range (AR) of (min, max)-amplitudes, the Amplitude Mean (AM), Amplitude Standard Deviation (ASD), Amplitude Unit (AU), map elevation (Z), Grid Interval (GI), and Contour Interval (CI). Shading and line contours are incremented by the CI, where the Thick Contour (TC) is the reference value for the line contours.

by the model. To facilitate south polar geological applications of earth gravity models, we consider below their development with particular emphasis on how they are constrained by Antarctic observations.

2. Earth gravity model predictions for the Antarctic

The EGM96 gravity predictions satisfy 30-arc-minute averages of marine gravity anomalies derived from satellite radar altimetry (Geos 3, Seasat, Geosat, ERS1 & 2), airborne gravity measurements and terrestrial gravity observations where available, and gravity anomalies computed from orbital analyses of 21 satellites using laser tracking data, GPS, Doppler data, and range-rate as well as satellite-to-satellite tracking and optical data (Lemoine *et al.*, 1998). Figure 2 classifies the gravity observations for the 30' Antarctic blocks south of 60°S that were used in the development of the EGM96 coefficients. Surface estimates, including those produced from satellite radar altimetry and airborne gravity observations are marked by grey-shaded regions, whereas the unsurveyed 30' blocks are marked by blank (white) areas.

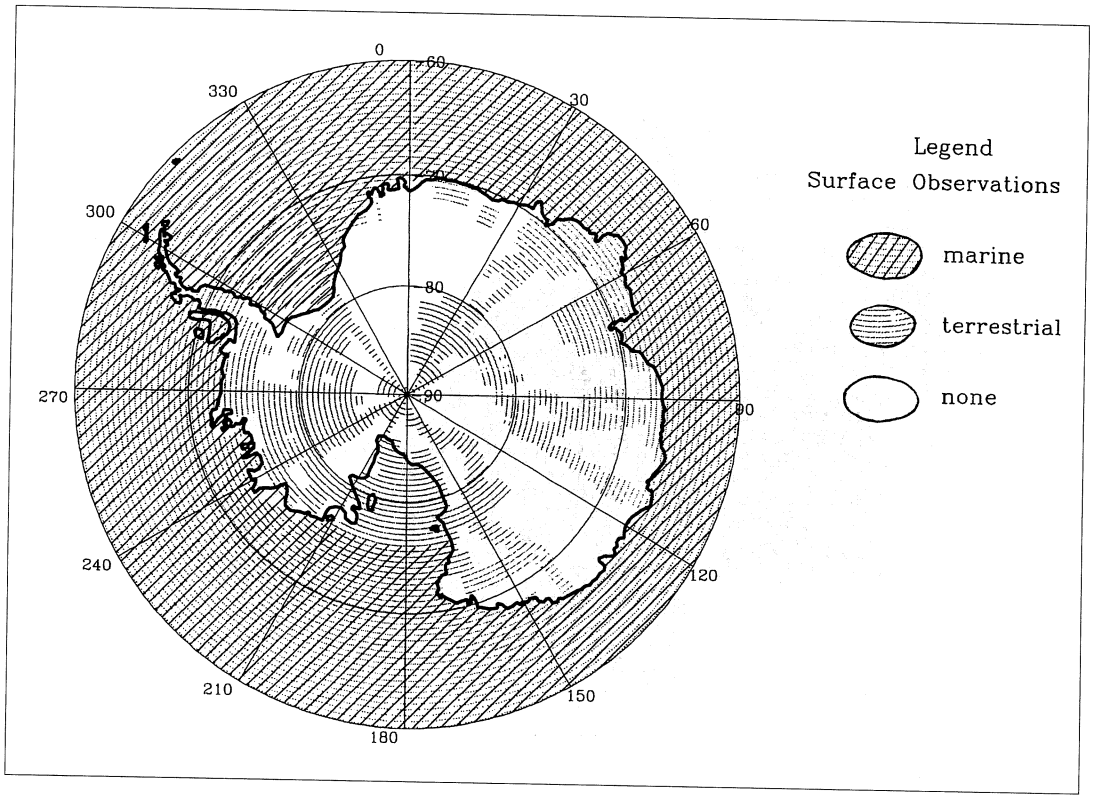

Fig. 2. Distribution of Antarctic 30' gravity anomaly averages used in developing the EGM96 coefficients. Ruled grey shading indicates the marine blocks constrained by satellite altimetry and, for the Weddel Sea, airborne gravity observations. Blocks constrained by surface gravity surveys are shaded grey, and unsurveyed blocks are unshaded (white). Anomaly averages in unsurveyed regions are constrained only by low-degree satellite-derived geopotential models and the topographic-isostatic potential implied by the Airy-Heiskanen hypothesis (Pavlis and Rapp, 1990).

Analysis of fig. 2 indicates that roughly 75% of these 30' blocks incorporate surface or airborne gravity observations. This coverage includes 91% of the marine blocks (diagonally ruled), 61% of the terrestrial blocks of Antarctica, 86% of the West Antarctic blocks, and nearly 50% of the East Antarctic blocks. Gravity estimates for unsurveyed blocks are constrained only by low-degree gravity predictions from satellite orbit analyses in combination with predictions of the topographic-isostatic potential based on the Airy-Heiskanen hypothesis (Pavlis and Rapp, 1990). Hence these anomaly estimates cannot be used for evaluating crustal isostatic properties because they incorporate the assumption of isostatic equilibrium.

The 30' block averages for producing the EGM96 spherical harmonic coefficients were generated in much the same manner as those of the previous 360 degree earth gravity model (Rapp *et al.*, 1991). Initially, a satellite-only model through degree 70 was derived for establishing the long wavelength properties of the block averages. The quality of the satellite-only model (EGM96S) was greatly improved by incorporating TOPEX/Poseidon orbital data determined from GPS tracking along with the Doppler (Tranet) tracking data of other satellites over the polar regions that were recently released by the U.S. Navy.

The satellite-only model was then modified by including altimetry and other near-surface

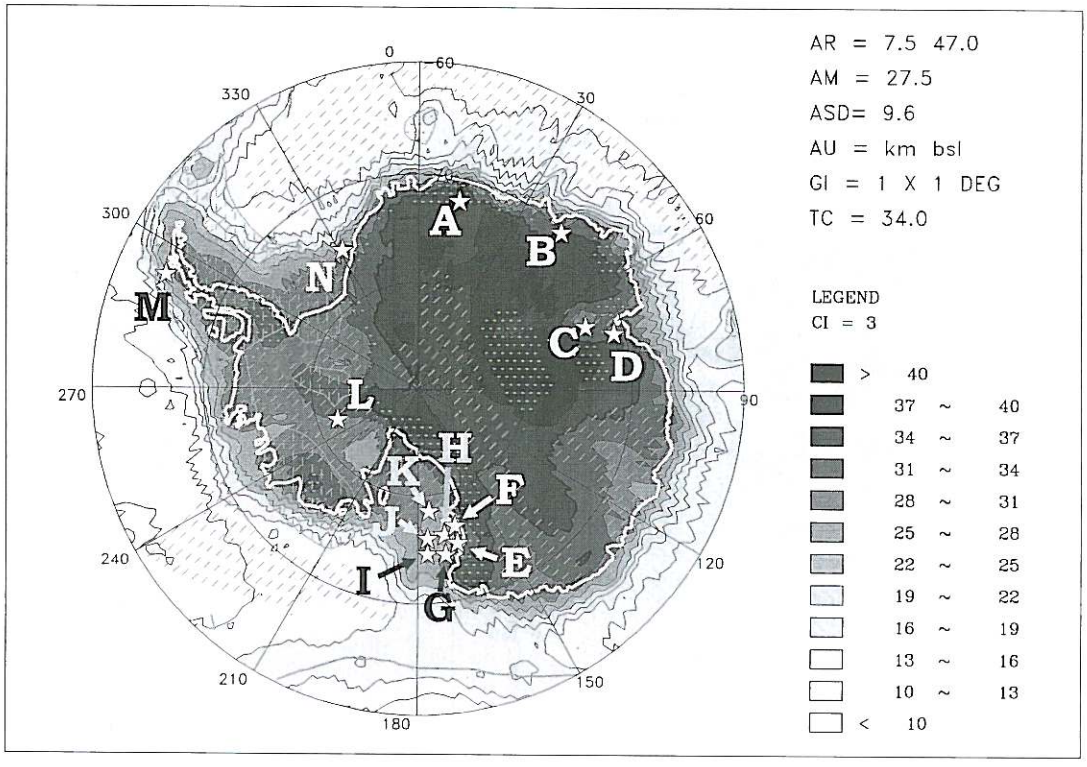

Fig. 3. Antarctic Moho depths estimated from correlating the FAGA of fig. 1 with the gravity effects of the terrain (von Frese *et al.*, 1997c). Generalized tectonic features and map annotations as listed for fig. 1 are also given. In addition, the distribution of large offset seismic estimates that are keyed to the seismic studies listed in table I are shown.

measurements to obtain an enhanced degree 70 combined-model. Newly available near-surface gravity data sets for Greenland, the former Soviet Union, South America, Asia, Africa and other regions have been incorporated into this combined analysis. Previous models were greatly limited because they had to rely on «geophysical» estimates of the block averages for these regions such as are required for the unsurveyed blocks of Antarctica. However, the inclusion of these new data sets along with satellite altimeter-implied marine free-air gravity anomalies put strong constraints on the nature of the gravity field within Antarctica, particularly at the longer wavelengths.

Finally, a banded diagonal matrix solution for degrees 71 to 359 and a quadrature solution for degree 360 were generated separately from the near-surface gravity estimates and merged with the degree 70 combined-model to yield a full 360 degree model. The predictions from the higher order harmonic coefficients were gridded with the predictions from the degree 70 combined-model into 30' averages from which a least squares solution for a 360 degree model was generated. It should be noted that since the input data sets were gridded into 30' mean anomalies, the maximum resolvable wavelength is 60' or about 111 km.

An example of the geological veracity of the EGM96 gravity predictions is given by von Frese *et al.* (1997c) who estimated the Antarctic Moho (fig. 3) from an analysis of the correlations between the free-air gravity anomalies (fig. 1) and an effective gravity model of the corresponding terrain. The results in fig. 3 are on average within about 7% of the available seismically determined estimates of the Antarctic Moho that are summarized in table I. The favorable comparison with the seismic Moho enhances our confidence in the use of EGM96 gravity predictions for Antarctic crustal studies. However, even an unfavorable comparison, such as might be observed by a future study, can yield insight on the Antarctic gravity field. In this case, the difference between the seismic- and gravity-determined Moho estimates could be modeled for the corresponding gravity effects to update the gravity field of the region and related earth models such as EGM96.

Table I. Comparison of Moho estimates from fig. 3 and large offset seismic studies. The distribution of these seismic studies as keyed to the listed references is also shown in fig. 3.

Seismic references	Seismic depths (km)	Figure 3 depths (km)
A) Kogan (1972)	38-40	37
B) Ikami *et al.* (1983); Ikami and Ito (1984, 1986)	40	34
C) Kurinin and Grikurov (1982)	25	31
D) Kurinin and Grikurov (1982)	30-40	32
E) McGinnis *et al.* (1983, 1985)	35	34
F) McGinnis *et al.* (1983, 1985)	28	29
G) von Frese *et al.* (1992)	20-25	24
H) Cooper *et al.* (1987)	18	24
I) Cooper *et al.* (1987)	21	24
J) Trehu *et al.* (1993)	17-20	25
K) ten Brink *et al.* (1993)	22-35	34
L) Clarke *et al.* (1997)	30	32
M) Guterch *et al.* (1985)	35-45	30
N) Petrik *et al.* (1983)	33-36	28

Considerable care must be taken in using the Antarctic EGM96 gravity predictions for geological applications because they are only marginally constrained by surface observations. Clearly, results such as the Moho estimates in fig. 3 would benefit greatly from additional gravity observations over the unsurveyed regions of Antarctica. However, significant and timely progress in acquiring these critical observations is likely to result only from satellite gravity surveys at low orbital altitudes (*i.e.*, 150-500 km) such as have been proposed for ESA's CHAMP (Reigber *et al.*, 1996) and NASA's GRACE (National Research Council, 1997) missions.

3. Satellite measurements of the gravity field

Satellites may be used to estimate the Earth's gravity field in either passive or active survey modes. Passive measurements involve tracking a satellite's orbit relative to the ground or to other satellites, whereas active measurements use satellite-generated electromagnetic pulses to image the geoid. Variations in both sets of measurements can be related to gravity field anomalies.

3.1. *Passive measurements*

Tracking the satellite in its orbit can determine the basal harmonic components of the Earth's gravity field. Satellite orbits are mostly a function of the lower order gravity harmonics and the effects of solar wind, lunar tidal forces, and other perturbing parameters (Kaula, 1966; Reigber, 1989). Depending on altitude, the satellite is primarily affected by the gravity harmonics through degree 20 or 30 with the power of the higher order harmonics tapering off to near zero through degree 70.

A model for predicting a satellite's location (C) may be calculated from *a priori* estimates of the above mentioned parameters (P_i) by

$$C = \sum_{i=1}^{n} P_i \,. \qquad (3.1)$$

As shown in fig. 4, differencing the calculated orbital location with the actual observed location (O) of the satellite yields a residual that is a function of both the errors in the model parameters (dP_i) and the observations (e_o). Rotations for various frames of reference must be determined as must the relationships between the orbital path and the various parameters used to predict the orbital path. Knowing these relationships, the difference between the actual location (as determined from observation) and the predicted location may be expressed by a well established observation equation (Kaula, 1966; Torge, 1989; Reigber, 1989) according to the general formula

$$(O-C) = \sum_{i=1}^{n} \frac{\partial C}{\partial P_i} \Delta P_i + e_o \,. \qquad (3.2)$$

An *a priori* model is assumed to be close to the ideal parameters, so that the desired corrections are small and may be linearized. With multiple (j) observations, this result becomes a linear system of equations that may be solved by least squares for the modifications (ΔP_i) to the parameters. This approach, however, involves tedious satellite tracking calculations and will also be limited over regions where satellite tracking data are lacking and hence had to be interpolated.

Additional refinements to this method have been offered (Lerch, 1991; Anderson and Cazenave, 1986; Lemoine *et al.*, 1998) that include schemes for weighting eq. (3.2) and adapting it for the gravity inversion of satellite-to-satellite tracking data. Satellite-to-satellite data in High-Low and Low-Low tracking configurations (fig. 5) provide more continuous coverage for determining the gravity field. In addition, the use of GPS for tracking satellites, such as in the case of the TOPEX/Poseidon mission, yield exceptionally good orbit determinations. However, these data still limit the solution of the gravity field to the lower order components that predominate at satellite altitudes.

3.2. *Active measurements*

Significantly higher order components of the Earth's anomalous gravity field can be mapped

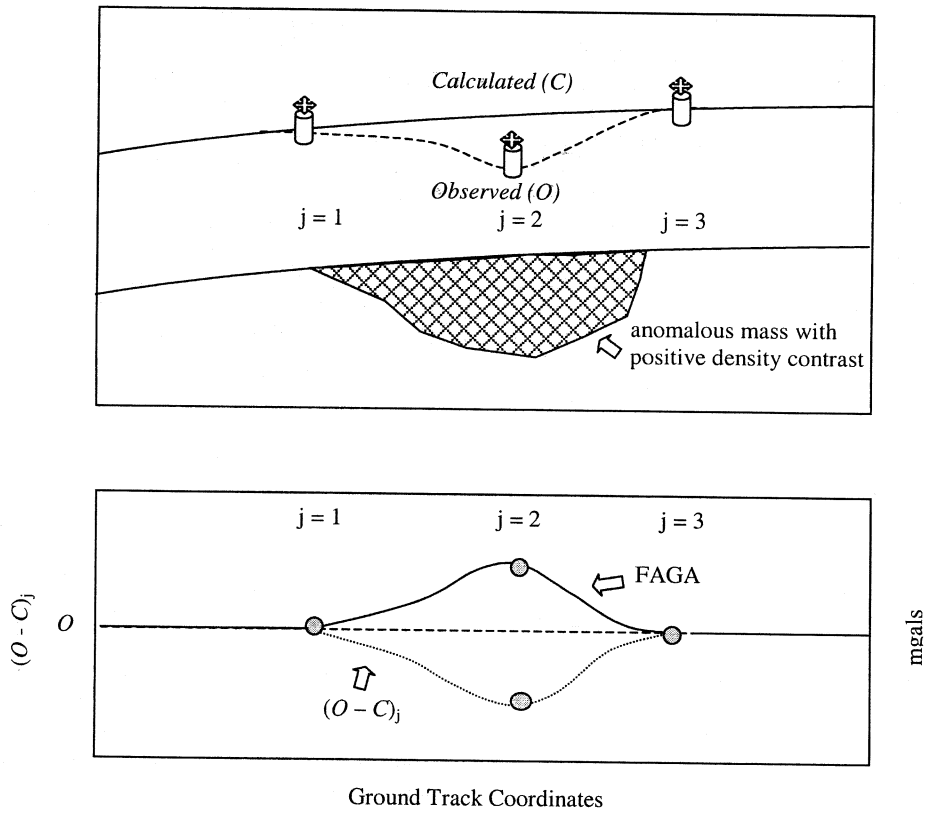

Fig. 4. Generalized gravity field measurement by ground-based tracking of a satellite. The displacement distance $(O\text{-}C)_j$ at location j is the difference between the calculated satellite orbital height (C) determined from *a priori* gravity field parameters and its observed height (O), which reflects the actual Earth with an anomalous mass of positive density contrast. Corrections (ΔP_i) to the a *priori* values are determined using eq. (3.2) to generate *a posteriori* parameters, which are used to estimate FAGA.

over the oceans using a satellite radar altimeter. The altimetry determines the distance from the satellite to the surface of the ocean (fig. 6) which serves as a proxy indicator of the Earth's geoid undulation. The geoid represents the effect of the disturbing potential at the Earth's surface, and therefore includes the higher order gravity components. By remotely measuring this surface with the radar, remarkably detailed and accurate gravity information may be retrieved for nearly 70% of the Earth.

The accuracy and resolution of altimetry-implied gravity anomalies are significantly limited by errors in determining the satellite orbits. Geodetic satellites commonly operate in inclined polar orbits where half of the ground tracks ascend from south to north across the Earth to intersect the other half that descend from north to south. The orbital mismatches at the cross-over points can be used to reduce satellite orbit errors significantly for optimal altimetry estimates of the gravity field (Kim, J.-H., 1996; Scharroo and Visser, 1998). The areal density of cross-over points increases dramatically towards the poles where the dense track coverage results in enhanced spatial resolution of the height

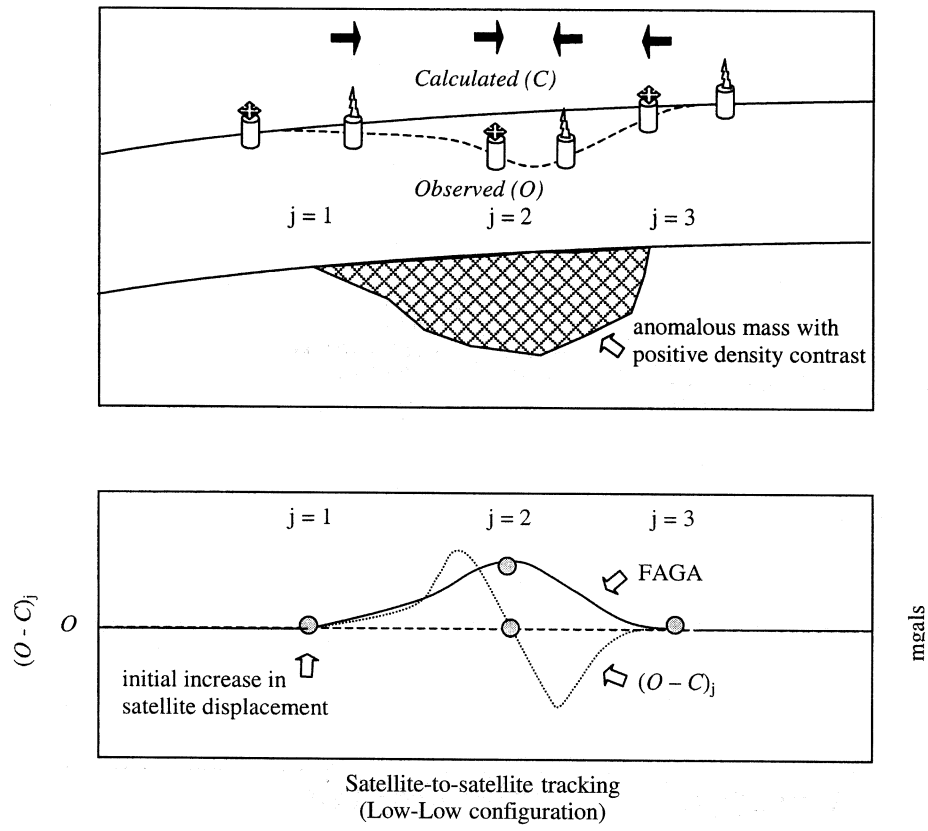

Fig. 5. Generalized gravity field measurement by satellite-to-satellite tracking in the Low-Low configuration. The fundamental observation at location j is the displacement distance $(O\text{-}C)_j$ between the satellites in the orbital plane. The calculated distance (C) is the difference between satellite positions in the absence of an anomalous mass as determined from *a priori* gravity field parameters. An anomalous mass with positive density contrast will cause the observed displacement (O) to increase at $j = 1$ as the leading satellite is pulled forward, then decrease at $j = 2$ as the trailing satellite surges forward while the leading satellite decelerates, and finally increase back to the initial displacement at $j = 3$ as the satellite pair moves beyond the anomalous mass effect. These changes in the displacement may be used in eq. (3.2) to refine the gravity field parameters and thereby estimate FAGA.

variations of the sea surface. For example, the Geosat data, which cover the southern oceans to 72°S, have an along-track data interval of roughly 7 km, whereas the spacing between tracks at 60°S is only about 2-3 km.

The observed altimetry data (ρ_{obs}) must first be screened and corrected for errors caused by the wet and dry troposphere, atmospheric pressure, the ionosphere, and other factors (fig. 6). The corrected altimetry data (ρ) may now be differenced with orbital elevations (H) determined from tracking and orbital models to generate Sea Surface Height (SSH) variations. Corrected SSH's are generated by applying models for other surficial factors such as the Static Sea Surface Topography (SSST) and performing a cross-over adjustment to reduce the Dynamic Sea Surface Topography (DSST) and orbit er-

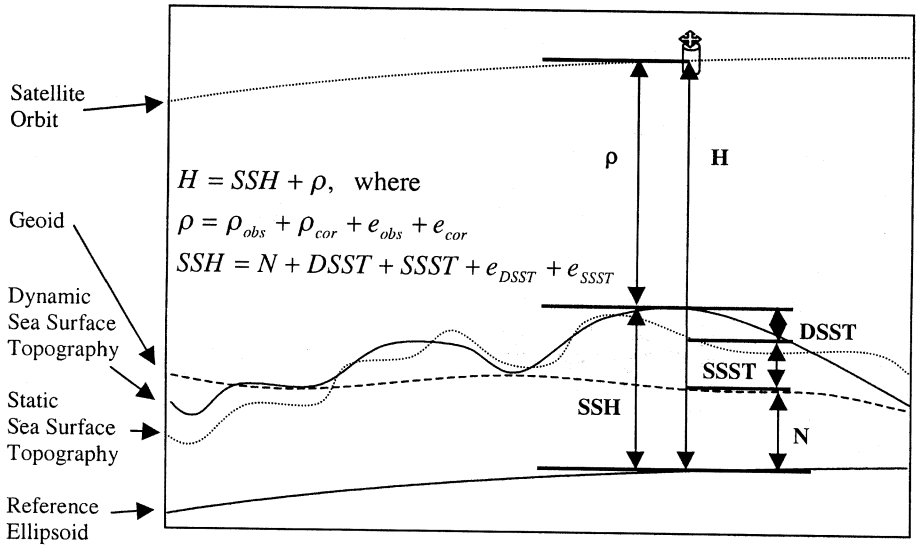

Fig. 6. Generalized gravity field measurement by satellite altimetry. Altimetry observations (ρ_{obs}) are corrected for various atmospheric effects (ρ_{cor}). The corrected altimetry data (ρ) are then differenced with the orbital heights (H) to generate Sea Surface Heights (SSH). Removal of the Dynamic Sea Surface Topography (DSST) and Static Sea Surface Topography (SSST) leaves the desired geoid undulations (N) that are converted into FAGA by the fundamental equation of geodesy (eq. 3.4).

rors arising in the determination of H. Models for correcting the (ρ_{obs}) and the SSH's are generally available with the altimetry data (*e.g.*, Kim, J.-H., 1996), so that the geoidal components may be readily recovered. It should be noted that the corrected SSH's contain residual effects and do not yet accurately reflect the geoid undulations at this point.

A common approach for extracting gravity anomalies from the corrected SSH's is to determine along-track vertical deflections from the descending and ascending orbits at the crossover points. These vertical deflections may be converted directly into gravity anomalies without the necessity of computing the geoid (Haxby *et al.*, 1983; Sandwell, 1992; McAdoo and Marks, 1992; Kim, J.-H., 1996; Sandwell and Smith, 1997). However, this procedure can mask the presence of residual orbit errors in the gravity anomaly predictions because of their shorter wavelength properties (Kim and von Frese, 1993; Kim, J.-H., 1996). Hence we evaluate the corrected SSH's directly for a geoid undulation model where the presence of orbit and other errors are more readily apparent.

We also impose strong geological constraints on our estimates of geoid undulations from the altimetry. For example, we divide the Geosat data into the two sets of subparallel ascending and descending tracking orbits. Lithospheric signals that are larger than the orbital track spacing (*i.e.*, roughly 2-3 km in the Antarctic) are coherent between two neighbouring tracks, and hence may be extracted with a spectral correlation filter (Kim, J.-H., 1996; von Frese *et al.*, 1997b). Inversely transforming the correlative wavenumber components from each data track yields geoid undulation estimates where noncorrelative features are suppressed, involving presumably crustal effects that are small compared to track spacing and nonlithospheric effects from temporal and spatial variations of ocean currents, measurement and data reduction errors, etc.

Separate geoids are now produced by gridding the correlation filtered ascending and descending data tracks. Typically, these geoid estimates exhibit strong washboard effects that parallel the orbital tracks and reflect errors in orbit determination, along-track data processing, and other nongeologic effects (Kim, J.-H., 1996; Kim, J.W. *et al.*, 1998). In the spectrum of each map, the track-line noise is restricted predominately to two of the quadrants with the other two being relatively uncontaminated. The pair of clean quadrants in one map is orthogonal to the clean pair of the other map because the track orientations of the ascending and descending data sets are different. Hence, a new spectrum can be constructed by combining the two pairs of clean quadrants to yield geoid undulation estimates where track-line noise is severely suppressed.

The resultant grid of geoid undulations (N) can be used to estimate Free-Air Gravity Anomalies (FAGA), because it is a function of the disturbing potential (T) as expressed in Bruns' formula (Heiskanen and Moritz, 1967)

$$T = N\gamma \tag{3.3}$$

where γ is normal gravity given by the International Gravity Formula for a standard Earth of homogeneous mass. Typically, geoid undulations are used to predict FAGA through the

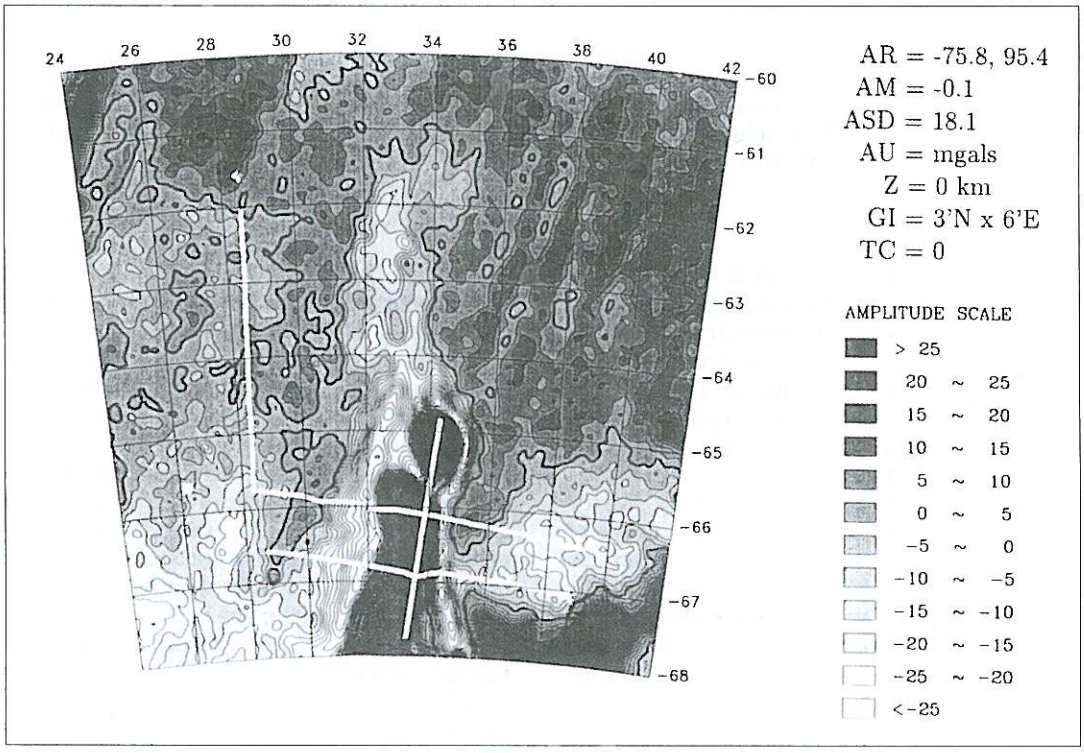

Fig. 7. Geosat altimetry-implied marine FAGA for the region of the Gunnerus Ridge that is located north of Japan's Syowa Station, Antarctica. Map annotations as listed for fig. 1 are given. Superimposed are four nearly straight segments of the 1990 cruise of the ship «Polarstern» along which the FAGA comparisons in figs. 8 and 9 were made.

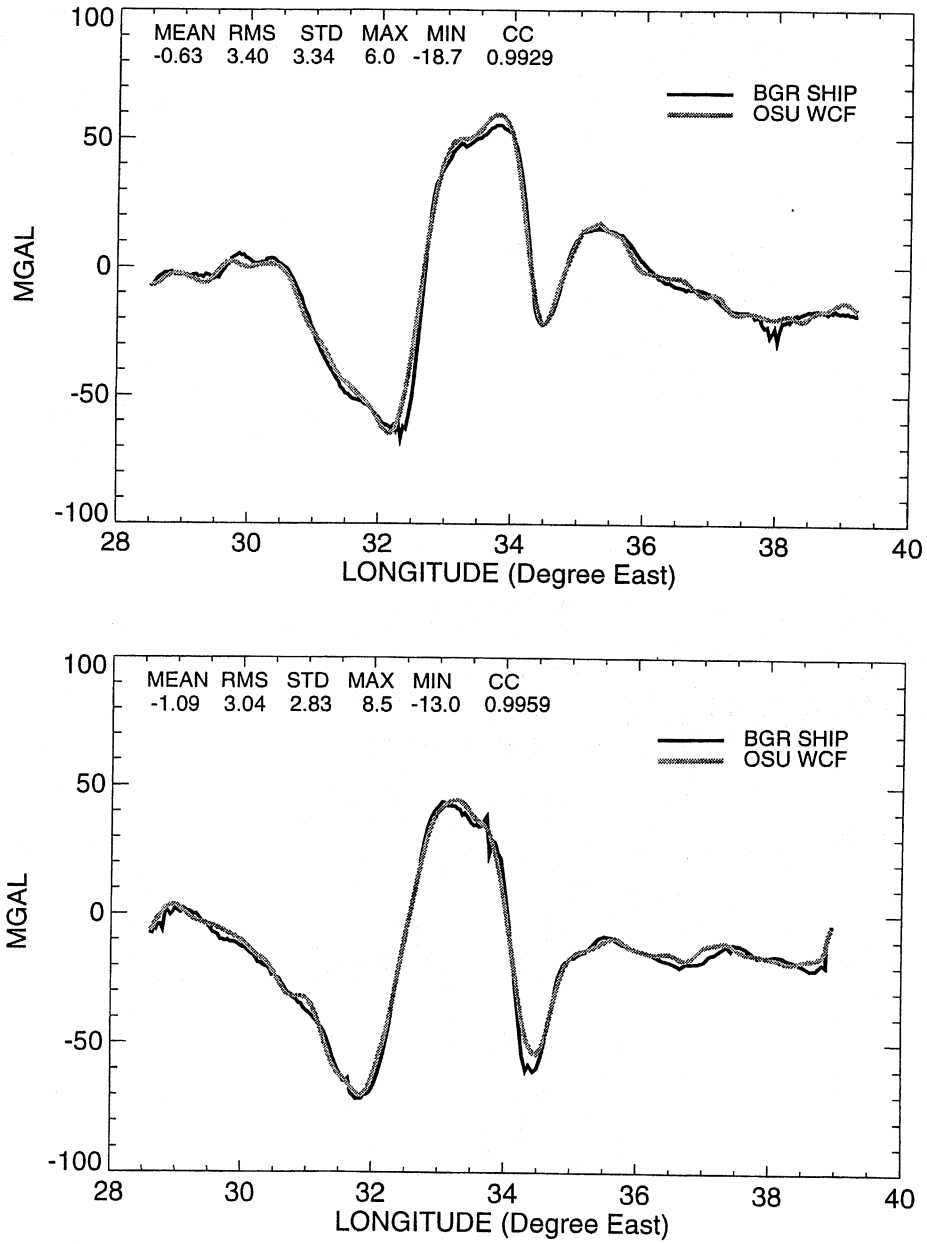

Fig. 8. FAGA comparisons between the ship measurements (BGR SHIP) and our wavenumber correlation filtered Geosat predictions (OSU WCF) along the west-east running tracks WE1 and WE2 that are located in fig. 7 near 66°S and 67°S, respectively. The statistics of their differences, which are given in the upper left corner of each profile comparison, include the mean (MEAN), root-mean-square (RMS), standard deviation (STD), maximum (MAX) and minimum (MIN) values. The coefficient of correlation (CC) between the two anomaly profiles is also given.

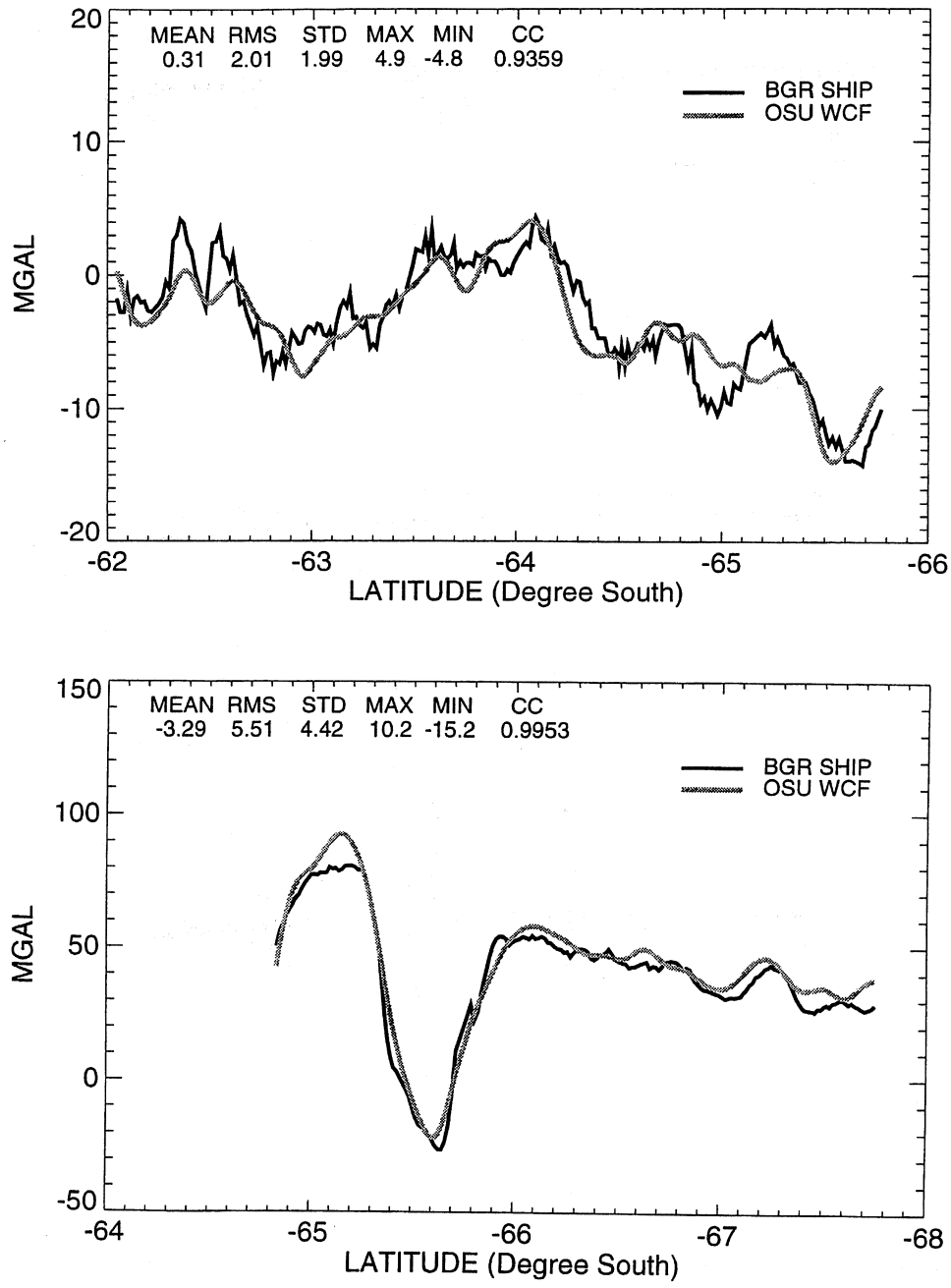

Fig. 9. FAGA comparisons between the ship measurements (BGR SHIP) and our wavenumber correlation filtered Geosat predictions (OSU WCF) along the north-south running tracks NS1 and NS2 that are located in fig. 7 near 28.5°E and 34°E, respectively. The statistics of their differences as listed in fig. 8 are also given.

fundamental equation of geodesy

$$\mathrm{FAGA} = -\frac{\partial T}{\partial r} - \frac{2T}{R} = -\frac{\partial (N\gamma)}{\partial r} - \frac{2(N\gamma)}{R} \qquad (3.4)$$

where R is the Earth's mean radius, and the radial (r) gradient of N is estimated by a spectral filter (Kim and von Frese, 1993; Kim, J.-H., 1996).

An example of Antarctic FAGA estimates at a grid interval of roughly 5 km from altimetry data of the Geosat mission is given in fig. 7 for the Gunnerus Ridge that is located offshore of Japan's Syowa Station. Insight on the errors in these FAGA predictions can be obtained by comparing them to good quality marine gravity measurements. The 1990 cruise of the ship «Polarstern», which was operated by the Bundesanstalt für Geowissenschaften und Rohstoffe (BGR), obtained accurate gravity data along the four nearly straight ship tracks that are superimposed on the FAGA predictions of fig. 7. The accuracy of the BGR data is estimated to be about 2 mgals or better from an analysis of the crossover points for these tracks and other tracks of the survey (Kim, J.-H., 1996).

The ship tracks considered in fig. 7 include the two roughly west-east running tracks WE1 and WE2 near 66°S and 67°S, respectively, and the two north-south running tracks NS1 and NS2 near 28.5°E and 34°E, respectively. The tracks WE1, WE2 and NS2 pass over areas of relatively great gravity relief, whereas track NS1 passes over a nearly flat gravity field. Because the cruise distance between gravity measurements was about 0.2 km, we considered the BGR data only at every tenth data point for this comparison. Accordingly, the number of data points considered ranged from 188 to 270 measurements per track over track lengths from 330 km to 490 km. The ship tracks investigated here are sufficiently long to check the Geosat predictions for any significant orbit biases and/or trends.

The free-air gravity anomaly comparisons between the ship measurements and our wavenumber correlation filtered Geosat predictions along the WE1 and WE2 tracks and NS1 and NS2 tracks are shown in figs. 8 and 9, respectively. This comparison illustrates the remarkable capacity of satellite altimetry to accurately map detailed features of the marine gravity field, even for regions such as considered here where the sea surface is relatively stormy and contaminated by floating ice. In general, our results are quite close to the theoretical accuracy limit of 3 mgals that was obtained by Sailor and Discoll (1993) for the Geosat data from a coherency analysis of hundreds of exact repeat orbits. Also, the coherence of the profiles appears well matched at 10 km and greater wavelengths (Kim, J.-H., 1996), which is slightly better than the 30 km wavelength estimates for Geosat given in Yale *et al.* (1995).

4. Conclusions

Satellite gravity observations provide important constraints on the lithospheric features and evolution of the Antarctic. Over relatively ice-free marine areas, available satellite altimetry yield free-air gravity anomaly estimates with wavelengths and accuracies approaching roughly 10 km and 3 mgals, respectively. Over terrestrial areas, EGM96 provides a geologically useful synthesis of available near-surface and satellite gravity observations up to wavelengths of about 1°. However, for large portions of East Antarctica, these predictions are constrained only to about degree 30 by direct gravity observations from satellites in orbits at altitudes of roughly 750 km and higher. Hence the pending CHAMP and GRACE missions at significantly lower altitudes (*e.g.*, 150-500 km) will provide results that will greatly improve our knowledge of the higher degree components of the Antarctic gravity field. Further insight on these components may be obtained by modeling the gravity effects of lithospheric mass variations that are imaged by seismic and other geophysical studies.

Acknowledgements

We thank H. Denker for making the gravity measurements from the BGR's 1990 cruise of the ship «Polarstern» available to us for the comparison reported in this study. Elements of

this investigation were produced with support from the NASA Goddard Space Flight Center under research grant NAG 5-2996, and the Ohio Supercomputer Center at The Ohio State University.

REFERENCES

ANDERSON, A.J. and A. CAZENAVE (1986): *Space Geodesy and Geodynamics* (Academic Press, Harcourt Brace Jovanovich Publ., New York).

CHANDLER, V.W., J.S. KOSKI, W.J. HINZE and L.W. BRAILE (1981): Analysis of multisource gravity and magnetic anomaly data sets by moving-window application of Poisson's theorem, *Geophysics*, **46**, 30-39.

CLARKE, T.S., P.O. BURKHOLDER, S.B. SMITHSON and C.R. BENTLEY (1997): Optimum seismic shooting and recording parameters and a preliminary crustal model for the Byrd Subglacial Basin, Antarctica, in *The Antarctic Region: Geological Evolution and Processes*, edited by C.A. RICCI (Terra Antarctica Publ., Siena), 485-493.

COOPER, A.K., F.J. DAVEY and G.R. COCHRANE (1987): Structure of extentionally rifed crust beneath the Western Ross Sea and Iselin Bank, Antarctica, from sonobuoy seismic data, in *The Antarctic Continental Margin Geology and Geophysics of the Western Ross Sea, Circum-Pacific Council for Energy and Natural Resour. Earth Sci. Ser., 5B, Houston, Tex.*, edited by A.K. COOPER and F.J. DAVEY, 93-118.

GUTERCH, A., M. GRAD, T. JANIK, E. PERCHUC and J. PAJCHEL (1985): Seismic studies of the crustal structure in West Antarctica 1979-1980 – Preliminary results, *Tectonophysics*, **114**, 411-429.

HAXBY, W.F., G.D. KARNER, J.L. LABRECQUE and J.K. WEISSEL (1983): Combined oceanic and continental data sets and their use in tectonic studies, American Geophysical Union, *Eos, Trans. Am. Geophys. Un.*, **64**, (52), 995-1004.

IKAMI, A. and K. ITO (1984): Deep crustal structure along the profile between Syowa and Mizuho Stations, East Antarctica, *Memoirs of the National Institute of Polar Research, Tokyo, Series C*, **15**, 19-28.

IKAMI, A. and K. ITO (1986): Crustal structure in the Mizuho Plateau, East Antarctica, by a two-dimensional ray approximation, *J. Geodyn.*, **6**, 271-283.

IKAMI, A., K. ITO, K. SHIBUYA and K. KAMINUMA (1983): Crustal structure of the Mizuho Plateau, Antarctica, revealed by explosion seismic measurements, in *Antarctic Earth Science – Proceedings of the Fourth International Symposium on Antarctic Earth Sciences (Adelaide, A; 16-20 August 1982)*, edited by R.L. OLIVER, P.R. JAMES and J.B. JAGO, Australian Academy of Science (Canberra-Cambridge University Press, Canberra), 509-513.

KAULA, W.M. (1966): *Theory of Satellite Geodesy* (Blaisdell Publ. Co., Waltham, MA).

KIM, J.-H. (1996): Improved recovery of gravity anomalies from dense altimeter data, *Department of Geodetic Science and Surveying Report #437*, The Ohio State University, Columbus.

KIM, J.-H. and R.R.B. VON FRESE (1993): Enhanced recovery of gravity field from satellite altimetry using geological constraints, *Eos, Trans. Am. Geophys. Un.*, **74**, 99.

KIM, J.W., J.-H. KIM, R.R.B. VON FRESE, D.R. ROMAN and K.C. JEZEK (1998): Spectral attenuation of track-line noise, *Geophys. Res. Lett.*, **25** (2), 187-190.

KOGAN, A.L. (1972): Results of deep seismic soundings of the Earth's crust in East Antarctica, in *Antarctic Geology and Geophysics - Symposium on Antarctic Geology and Solid Earth Geophysics (Oslo, S; 6-15 August 1970)*, edited by R.J. ADIE (Universitetsforlaget, Oslo), 485-489.

KURININ, R.G. and G.E. GRIKUROV (1982): Crustal structure of part of East Antarctica from geophysical data, in *Antarctic Geoscience - Symposium on Antarctic Geology and Geophysics (Madison, WI, USA; 22-27 August 1977)*, edited by C. CRADDOCK (University of Wisconsin Press, Madison), 919-923.

LEMOINE, F.G., S.C. KENYON, J.K. FACTOR, R.G. TRIMMER, N.K. PAVLIS, D.S CHINN, C.M. COX, S.M. KLOSKO, S.B. LUTHCKE, M.H. TORRENCE, Y.M. WANG, R.G. WILLIAMSON, E.C. PAVLIS, R.H. RAPP and T.R. OLSON (1998): The development of the joint NASA GSFC and National Imagery and Mapping Agency (NIMA) Geopotential Model EGM96, *NASA/TP-1998-206861* (Goddard Space Flight Center, Greenbelt).

LERCH, F.J. (1991): Optimum weighting and error calibration for estimation of gravitational parameters, *Bull. Geod.*, **65**, 44-52.

MCADOO, D.C. and K.M. MARKS (1992): Gravity field of the southern ocean from Geosat data, *J. Geophys. Res.*, **96** (B3), 3247-3260.

MCGINNIS, L.D., D.D. WILSON, W.J. BURDELIK and T.H. LARSON (1983): Crust and upper mantle study of McMurdo Sound, in *Antarctic Earth Science - Proceedings of the Fourth International Symposium on Antarctic Earth Sciences (Adelaide, A; 16-20 August 1982)*, edited by R.L. OLIVER, P.R. JAMES and J.B. JAGO (Australian Academy of Sciences, Canberra-Cambridge University Press, Canberra), 204-208.

MCGINNIS, L.D., R.H. BOWEN, J.M. ERICKSON, B.J. ALLRED and J.L. KREAMER (1985): East-West Antarctic boundary in McMurdo Sound, *Tectonophysics*, **114**, 341-356.

NATIONAL RESEARCH COUNCIL (1997): *Satellite Gravity and the Geosphere: Contributions to the Study of the Solid Earth and its Fluid Envelope* (National Academy Press, Washington D.C.).

PAVLIS, N.K. and R.H. RAPP (1990): The development of an isostatic gravitational model to degree 360 and its use in global gravity modeling, *Geophys. J. Int.*, **100**, 369-378.

PETRIK, G.V., V.N. SERGEEV and A.L. KOGAN (1983): Deep seismic studies of the Western Antarctic, *Soviet Geology and Geophysics*, **23**, 99-106.

RAPP, R.H., Y.M. YANG and N.K. PAVLIS (1991): The Ohio State 1991 geopotential and sea surface topography harmonic coefficient models, *Dept. of Geodetic Science*

and Surveying Report #410, The Ohio State University, Columbus.

REIGBER, C. (1989): Gravity field recovery from satellite tracking data, in *Theory of Satellite Geodesy and Gravity Field Determination*, edited by F. SANSÒ and R. RUMMEL (Springer-Verlag, Berlin).

REIGBER, C., R. BOCK, C. FÖRSTE, L. GRUNWALDT, N. JAKOWSKI, H. LÜHR, P. SCHWINTZER and C. TILGNER (1996): CHAMP phase B executive summary, *Scientific Technical Report STR96/13*, Geoforschungs-Zentrum-Potsdam, Potsdam.

SAILOR, R.V. and M.L. DISCOLL (1993): Noise models for satellite altimeter data, *Eos, Trans. Am. Geophys. Un.*, **74**, 99.

SANDWELL, D.T. (1992): Antarctica marine gravity field from high-density satellite altimetry, *Geophys. J. Int.*, **109**, 437-448.

SANDWELL, D.T. and W.H.F. SMITH (1997): Marine gravity anomalies from Geosat and ERS-1 satellite altimetry, *J. Geophys. Res.*, **102** (B5), 10039-10054.

SCHARROO, R. and P. VISSER (1998): Precise orbit deter-mination and gravity field improvement for the ERS satellites, *J. Geophys. Res.*, **102** (C4), 8113-8127.

TEN BRINK, U.S., B.C. BEAUDOIN and T.A. STERN (1993): Geophysical investigations of the tectonic boundary between East and West Antarctica, *Science*, **261**, 45-50.

TORGE, W. (1989): *Gravimetry* (Walter de Gruyter Press, New York).

TREHU, A.M., J.C. BEHRENDT and J.C. FRITSCH (1993): Crustal structure of the Central Basin, Ross Sea, Antarctica, *Geologisches Jahrb., Reihe E, 47*, edited by D. DAMASKE and J.C. FRITSCH (GANOVEX V), 291-312.

VON FRESE, R.R.B., W.J. HINZE and L.W. BRAILE (1982): Regional North American gravity and magnetic anomaly correlations, *Geophys. J. R. Astron. Soc.*, **69**, 745-761.

VON FRESE, R.R.B., D.E. ALSDORF, J.-H. KIM, T.M. STEPP, D.R.H. O'CONNELL, K.J. HAYDEN and W.S. LI (1992): Regional geophysical imaging of the Antarctic lithosphere, in *Recent Progress in Antarctic Earth Science*, edited by Y. YOSHIDA, K. KAMINUMA and K. SHIRAISHI (Terrapub, Tokyo), 465-474.

VON FRESE, R.R.B., M.B. JONES, J.W. KIM and W.S. LI (1997a): Spectral correlation of magnetic and gravity anomalies of Ohio, *Geophysics*, **62**, 365-380.

VON FRESE, R.R.B., M.B. JONES, J.W. KIM and J.-H. KIM (1997b): Analysis of anomaly correlations, *Geophysics*, **62**, 342-351.

VON FRESE, R.R.B., J.W. KIM and L. TAN (1997c): Crustal analysis of spectrally correlated terrain gravity effects and free-air gravity anomalies, *Eos, Trans. Am. Geophys. Un.*, **78**, S119.

VON FRESE, R.R.B., H.R. KIM, L. TAN, J.W. KIM, P.T. TAYLOR, M.E. PURUCKER, D.E. ALSDORF and C.A. RAYMOND (1999): Satellite magnetic anomalies of the Antarctic crust, *Ann. Geofis.*, **42** (2), 309-326 (this volume).

YALE, M.M., D.T. SANDWELL and W.H.F. SMITH (1995): Comparison of along-track resolution of stacked Geosat, ERS-1, and TOPEX satellite altimeters, *J. Geophys. Res.*, **100** (B8), 15117-15127.